SPIRAL GALAXIES AND THE PECULIAR VELOCITY FIELD

RICCARDO GIOVANELLI AND MARTHA P. HAYNES
Cornell University, Ithaca, NY, USA

PIERRE CHAMARAUX
Observatoire de Meudon, Meudon, France

LUIZ N. DA COSTA
Observatorio Nacional, Rio de Janeiro, Brazil
and Institut d'Astrophysique, Paris, France

WOLFRAM FREUDLING
ESO ST–European Coordinating Facility, Garching, Germany

JOHN J. SALZER
Wesleyan University, Middletown, CT, USA

AND

GARY WEGNER
Dartmouth College, Hanover, NH, USA

Abstract.

We report results of a redshift–independent distance measurement survey that extends to all sky and out to a redshift of approximately 7500 km s^{-1} . Tully–Fisher (TF) distances for a homogeneous sample of 1600 late spiral galaxies are used to analyze the peculiar velocity field. We find large peculiar velocities in the neighborhood of superclusters, such as Perseus–Pisces (PP) and Hydra–Centaurus, but the main clusters embedded in those regions appear to be virtually at rest in the CMB reference frame. We find no compelling evidence for large–scale bulk flows, whereby the Local Group, Hydra–Cen and PP would share a motion of several hundred km s^{-1} with respect to the CMB. Denser sampling in the PP region allows a clear detection of infall and backflow motions, which can be used to map the mass distribution in the supercluster and to obtain an estimate of the cosmological density parameter.

M. Kafatos and Y. Kondo (eds.), Examining the Big Bang and Diffuse Background Radiations, 183–191.

1. Introduction

The discovery of the dipole anisotropy of the Cosmic Microwave Background (CMB) has been widely interpreted as a Doppler effect, resulting from the motion of the Local Group with respect to the comoving reference frame at a velocity of 620 km s^{-1} in the direction $l = 270 \pm 5$, $b = 30 \pm 3$ (Kogut et al. 1993). The independent measurement of redshifts and distances for individual galaxies, which can be assumed to be fair tracers of the peculiar velocity field, provides a test for the Doppler interpretation of the CMB dipole and an estimate of the distribution of masses whose gravitational effects give rise to the peculiar motion field. After the early measurements of the infall of the Local Group in the Local Supercluster (Aaronson et al. 1982), the existence of a larger attractor was independently postulated by Shaya (1984), Tammann and Sandage (1985) and Lilje et al. (1986) to coincide with the Hydra–Centaurus supercluster. The measurements of Lynden–Bell et al. (1987) suggested the existence of an even larger, somewhat more distant mass perturber, at an approximate $cz \simeq 4300$ km s^{-1} . Scaramella et al. (1989) made the radical suggestion that much of the perturbation responsible for the LG motion could arise from the Shapley Supercluster at $cz \simeq 14,000$ km s^{-1} . The TF distance measurements reported by several groups (Willick 1991, Mathewson et al. 1991, Courteau et al. 1993) and the dipole of the distribution of cluster brightest ellipticals (Lauer and Postman 1994) lent credence to a scenario where the large–scale bulk flows extend over distances comparable to that of the Shapley Supercluster. These results were in conflict with the relatively smaller convergence depth predicted from the redshift distribution of IRAS galaxies (Strauss et al. 1992). It is also somewhat disconcerting that, amidst reported bulk flows of several hundred km s^{-1} and the dramatic density contrast in the light distribution, as emphasized by redshift surveys, very small gradients in the peculiar velocity flow would be detected within the 7,000 km s^{-1} or so radius of the sphere sampled by TF studies. In this paper, we shall report results that are discrepant with previous TF studies, favoring a picture of the local universe characterized by a small convergence depth.

2. Samples Used

The results presented in the following sections are drawn from several data sets, namely: (a) a sample of 1500 Sbc–Sc galaxies of Dec. $> -45°$ and $cz < 7500$ km s^{-1} , restricted to objects with blue visual diameters $> 1.3'$ (hereinafter referred to as the Sc sample); (b) a survey of the PP supercluster extending to $cz \simeq 12,000$ km s^{-1} and angular size $> 0.8'$ which includes an additional 300 objects to those in sample (a) (the PP sample);

https://doi.org/10.1017/S007418090011006X Published online by Cambridge University Press

(c) a cluster sample, including spiral galaxies in 20 clusters to $cz \simeq 12,000$ km s^{-1} , and the addition of 300 objects to those in samples (a) and (b). For each of these galaxies, we have obtained I band CCD images and high quality velocity widths. For samples (a) and (b), velocity widths derive from 21cm observations made at Arecibo, Nançay, Green Bank and Effelsberg; for sample (c), additional velocity widths were obtained from optical spectra taken at the 5m telescope on Mt. Palomar, in collaboration with T. Herter and N. Vogt. The I band observations were carried out at MDM, Kitt Peak, CTIO and ESO telescopes. More details on the selection criteria of the (a) and (b) samples, including their mean photometric characteristics, can be found in Giovanelli et al. (1994, 1995).

In order to achieve full sky coverage with the Sc sample, our data were combined with those of Mathewson et al. (1992) in the South polar cap, after selection through a homogeneous set of criteria that would allow smooth merger into our sample and reprocessing of their data with the same procedures applied to ours. After filtering the sample for duplicate entries, objects with inadequate parameters for TF use, poor photometry, dwarf and interacting systems, etc, we obtain an all sky Sc sample of 1600 galaxies.

3. Corrections Applied to Observed Parameters

The main parameters entering our estimate of a TF distance are the total I band magnitudes, disk inclinations and velocity widths. Several corrections need to be applied to the observed quantities, before they can be used as diagnostic tools, namely those for galactic, cosmological and internal extinction effects to magnitudes; cosmological, instrumental, turbulent and inclination corrections for the widths; seeing and bulge contamination for disk inclinations.

While typical photometric accuracy inferred from CCD images is on the order of a few percent, corrections as applied by different groups may differ by several tenths of a mag. In Giovanelli et al. (1994) we have reviewed the procedures for the internal extinction corrections, and in Giovanelli et al. (1995) we present a luminosity dependent solution for that problem. In fig. 1, we illustrate an important result of those studies: if the correction to the observed total magnitude m for conversion to a standard m° face–on aspect is $m - m^\circ = \gamma \log(a/b)$, where a/b is the disk axial ratio inferred from the ellipticity of the outer isophotes, then γ is found to be luminosity dependent. Its value varies between 0.5 and 1.2, higher for the more luminous galaxies. These are substantially higher values than adopted in most previous TF applications. It is clear that a luminosity dependence of γ will affect the inferred slope of the TF relation. In Giovanelli et al. (1995) we discuss how

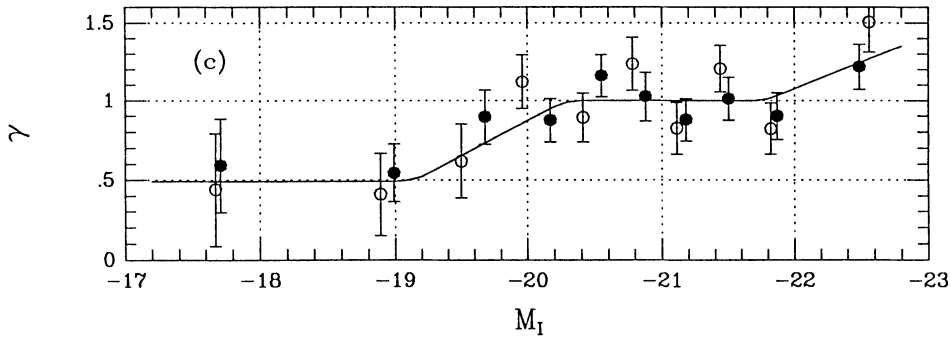

Figure 1. Luminosity dependence of the slope coefficient γ for the internal extinction law: $m - m^{\circ} = \gamma \log(a/b)$.

an inadequate extinction correction law can produce unwanted effects in the computation of peculiar velocity, such as spurious dependences of the latter on both luminosity and inclination.

Particular attention has been applied to the measurement and the processing of velocity widths, as the associated errors are a very important component of observational scatter in the TF relation, especially for galaxies of smaller velocity widths. Twenty–one cm velocity widths reported in the literature are often measured on heavily smoothed line profiles, as they pertain to low S/N observations optimized for redshift determination. We have reobserved a large fraction of those in order to obtain reliable widths, and have optimized width measurement algorithms that take into consideration line shape, S/N and resolution of the data.

4. Template for the TF Relation

The adoption of a TF template relation is perhaps the most delicate step in a peculiar velocity measurement program. A relation with the wrong offset or slope will produce a spurious peculiar velocity field with a characteristic geocentric signature. In a sample with partial sky coverage, it can easily mimic a bulk flow. The fit to a single cluster of galaxies is subject to the vagaries of small number statistics, and when the resulting TF relation is used as a template, it is likely to produce spurious results. We have thus chosen to use our cluster sample (see list in Table 1) to produce a TF template relation. The first step in such process regards cluster membership. Two different set of membership criteria were applied, producing a "strict

TABLE 1

CLUSTERS USED IN TEMPLATE

Cluster	R.A.	Decl.	V_{cmb} km s^{-1}	V_{pec} this paper	V_{pec} HM [a]	V_{pec} MFB [b]	N_{tot}	N_{in}
N507	012000.0	+330400	4741	+207±165	+76±296		22	10
A 262	014950.0	+355440	4574	0±140	-576±391		27	13
A 400	025500.0	+055000	6842	-224±190	-130±537		27	9
Fornax	033634.0	-353642	1260	-305±45		-58	35	17
Cancer – a	051353.7	+062441	4886	+20±90	-104±377		48	13
Antlia	102745.0	-350411	3134	+318±98	+324±223	+781	20	18
Hydra=A1060	103427.7	-271626	4085	-75±115	+184±296	+311	35	19
A1367	114154.0	+200700	6750	+94±112	-255±431		39	25
UMa	115400.0	+493000	1091	+523±50			31	26
Cen30	124606.0	-410200	3378	+266±110	+509±213	+997	22	22
Coma=A1656	125724.0	+281500	7225		+80±428		53	30
ESO508	130954.0	-230854	3276	+355±170	+654±206	+671	16	8
Kl 27=A3574	134606.0	-300900	4888	+207±160		+368	22	9
A2199	162654.0	+393800	9058	0±255			23	9
Pavo I	201300.0	-710000	4104	-19±160		+661	23	
Pegasus	231742.6	+075557	3958	-290±105	-588±285		34	12
A2634	233554.9	+264419	9483	-206±200	-906±639		41	19

[a] Han & Mould 1992, *Ap. J.* **396**, 453

[b] Mathewson, Ford & Buchhorn 1992, *Ap. J. Suppl. Ser.* **81**, 413

members sample" whereby only galaxies within 2 Abell radii and within a conservative $\Omega = 0.25$ caustic from the cluster center were chosen, and an "extended sample" which includes nearby supercluster members out to 4 Abell radii. The strict sample contains 260 galaxies and the extended one, 525. The corresponding TF relations differ very little from each other. TF diagrams $(M, \log W)$ were built for each individual cluster and combined into a composite by shifting in M, taking into account each cluster's incompleteness correction. The magnitude shift for each cluster necessary to match the composite template yields a relative distance modulus and was χ^2–computed simultaneously with the determination of the optimal TF slope for the composite sample. The magnitude scatter in the composite TF relation is 0.29 mag.

The slope of the TF relation is best determined by a sample that maximizes the dynamic range in $(M + 5\log h, \log W)$, i.e. one that preferentially includes nearby clusters. On the other hand, the magnitude offset ("zero point", a relative concept as long as the value of h isn't specified) of the relation is best obtained from a sample of distant clusters for which a motion of given amplitude in km s^{-1} translates into a small magnitude shift and for which the physical size of the cluster is small in comparison to its

https://doi.org/10.1017/S007418090011006X Published online by Cambridge University Press

mean distance.

The magnitude zero–point of our TF relation was adopted as that of the mean relation obtained from the subset of most distant clusters in the sample ($cz > 4000$ km s^{-1}) as seen by an observer at rest with respect to the CMB. This is our closest operational definition of a CMB rest reference frame. Even if the clusters partook of very large scale bulk motion, their mean TF relation would define a reference frame at rest with respect to the CMB, provided that their sky distribution is relatively isotropic. The use of the distant clusters rather than the whole cluster sample for this purpose allows for the smallest margin of error in the approximation of a CMB rest frame by our TF template. Individual cluster peculiar velocities with respect to that frame and associated errors (estimated using galaxies in the extended sample) are listed in Table 1. These are preliminary values, and small changes resulting from refinements in the analysis are likely to apply. For those clusters for which other estimates of peculiar velocity by Han and Mould (1992) or Mathewson et al. (1992) are available, a comparison is possible. Note that if the distant clusters partook of large scale bulk flow, their individual velocities would reflect it. Instead, indications are that they are individually at rest with respect to the CMB. Large velocities are measurable for nearby clusters, indicating that they partly share in the LG motion with respect to the CMB.

5. The Peculiar Velocity Field of the Sc Sample

Figure 2 gives two representations of the peculiar velocity field as obtained from the all sky Sc sample. In the top panel, the peculiar velocities are given in the Local Group reference frame, i.e. $V_{pec} = V_{LG} - V_{TF}$, where V_{LG} is the radial velocity measured with respect to the LG, and V_{TF} that predicted by the velocity width and apparent magnitude of the galaxy. In the bottom panel, peculiar velocities are given in the CMB reference frame. The redshift depth of the Sc sample is 7500 km s^{-1} . In the top panel we see the motion of the LG with respect to the CMB reflected in the prevalence of positive peculiar velocities in the southern galactic hemisphere and of negative ones in the northern hemisphere. The apex of the CMB dipole is at roughly (10.5^h,$-25°$). The dipole signature largely disappears in the bottom panel, when the peculiar velocity field is referred to the CMB. This immediately tells us that the majority of galaxies in the sample do not partake of the LG motion with respect to the CMB.

In a quantitative way, the immediately preceding statement is illustrated in Table 2, where the apex location and the amplitude of the dipole of the peculiar velocity field is displayed separately for galaxies within different redshift shells. The first line refers to all galaxies in the all sky Sc sample: a

https://doi.org/10.1017/S007418090011006X Published online by Cambridge University Press

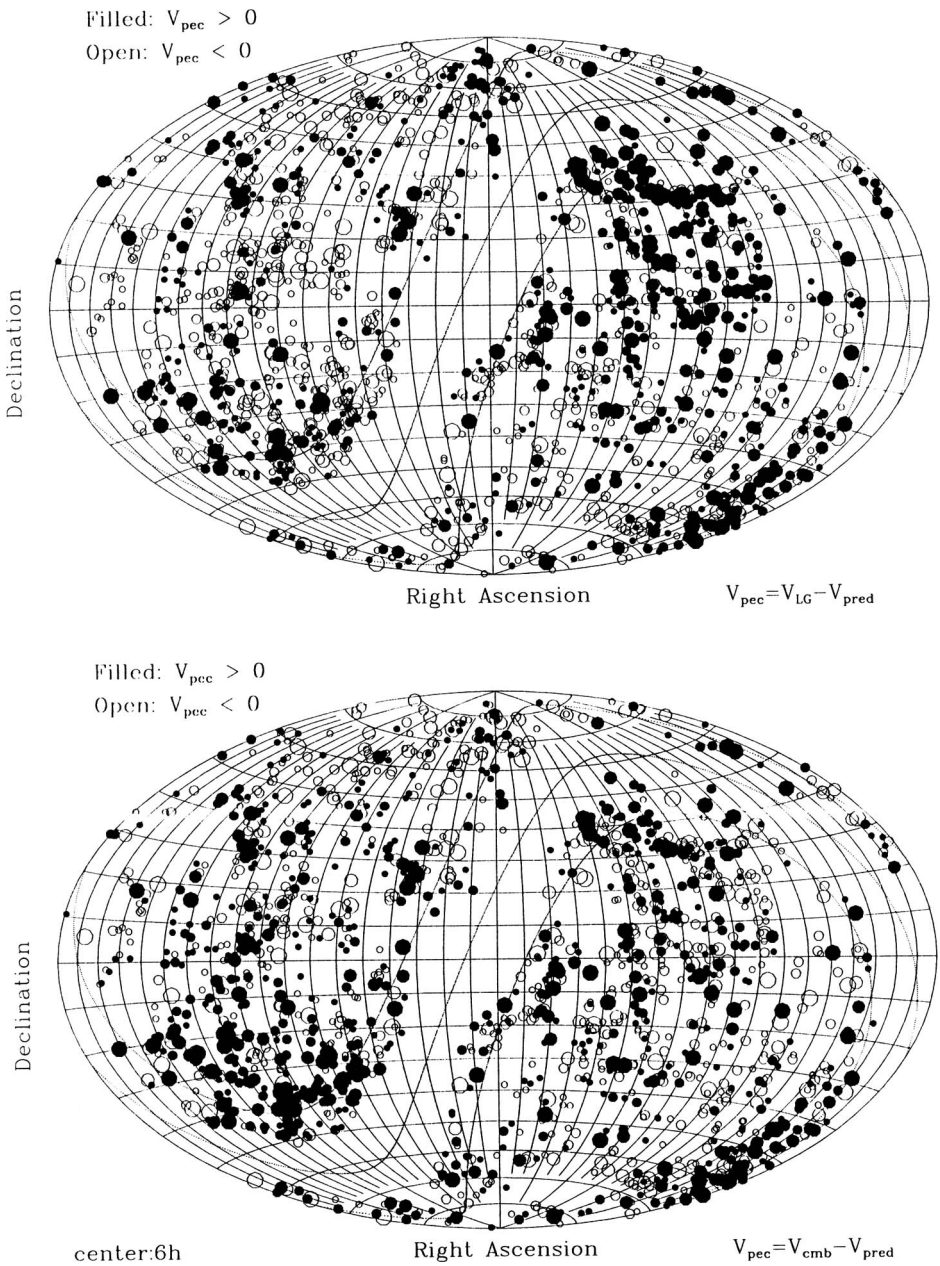

Figure 2. Peculiar velocities of galaxies in the all sky Sc sample. Each symbol represents a galaxy, of which 1600 are plotted. Filled symbols are positive (receding) and open symbols negative velocities. The coordinate system is equatorial, with (R.A., Dec.)=(6^h, 0°) at the center; "meridians" are each 40^m and "parallels" each 10°. Dotted lines are plotted for galactic $b = 0°$ and $b = \pm 20°$. The location of the apex of the CMB dipole is approximately at (R.A., Dec.)=(10.5^h, -25°). In the top panel velocities are referred to the LG reference frame; in the bottom, to the CMB.

https://doi.org/10.1017/S007418090011006X Published online by Cambridge University Press

TABLE 2

DIPOLES OF THE PECULIAR VELOCITY FIELD

V_{cmb} Window	$V_{pec}(LG)$	l	b	# Gals.
All	417±28	253±9	37±3	1585
2000–3000 km s^{-1}	333±41	268±16	41±8	235
3000–4000 km s^{-1}	437±57	242±20	24±5	303
4000–5000 km s^{-1}	551±62	236±24	37±5	372
5000–6000 km s^{-1}	566±81	281±15	24±25	270
CMB	627±22	276±3	30±3	*

*KOGUT et al. 1993, *Ap. J.* **419**, 1

net bulk flow of about 200 km s^{-1} is detectable. As the sample is separated in redshift shells, we see that both the apex and the amplitude of the motion converge towards that implied by the CMB temperature anisotropy. By the time the shell has reached a radius of about 5000 km s^{-1} , galaxies contained within it are essentially at rest with respect to the CMB.

In contrast, the peculiar velocity field in the vicinity of large concentrations of galaxies, such as the Hydra–Centaurus and the Perseus–Pisces superclusters appears quite disturbed. Infall and backflow velocities are seen rising to about 1300 km s^{-1} , at distances of about 2000 km s^{-1} of the center of those features. At the same time, the centers of mass of those agglomerates appear to be virtually at rest with respect to the CMB. The amplitude of the peculiar motions around superclusters is consistent with expectations based on redshift surveys and suggest that the light and matter distributions are not strongly biased. Preliminary estimates of the cosmological density suggest values of $\Omega^{0.6}/b \sim 1$, where b is the bias parameter between the galaxian and mass density distributions.

The motion of the LG with respect to the CMB arises from the joint attraction of the large mass concentration represented by Hydra–Cen, neighboring clusters and Virgo, and the virtual repulsion of the large void extending between the LG and the PP supercluster. The Hydra–Cen region does not exhibit a significant motion with respect to the CMB.

In summary, our results indicate that the region enclosed within a 7500 km s^{-1} radius exhibits a mild bulk flow of about 200 km s^{-1} ; this arises from the asymmetry of the mass distribution in the local universe and the location of the LG in a region characterized by a large mass density gradient. The central regions of the large "attractors" — the Hydra–Cen and PP superclusters — are at rest with respect to the CMB and *do not*

https://doi.org/10.1017/S007418090011006X Published online by Cambridge University Press

partake of large scale bulk flow. The convergence depth is on the order of 5000 km s^{-1} .

The discrepancy of our results with those of other TF studies arise principally from the merits of (a) access to an all–sky, homogeneous sample, (b) a different TF template relation, which is based on a very extensive study of clusters, and (c) an internal extinction correction that allows for larger flux corrections and is luminosity dependent.

This work was supported by NSF grants AST91-15459, AST92-18038 and AST90-23450. It is based on observations made at the National Astronomy and Ionosphere Center, the National Radio Astronomy Observatory and the National Optical Astronomical Obervatories, which are operated respectively by Cornell University, Associated Universities, Inc. and Associated Universities for Research in Astronomy, under cooperative agreements with the National Science Foundation.

References

1. Aaronson, M., Huchra, J., Mould, J., Schechter, P.L. and Tully, R.B. (1982) *Ap. J.* **258**, 64
2. Courteau, S., Faber, S.M., Dressler, A. and Willick, J.A. (1993), *Ap. J. (Letters)* **412**, L51
3. Giovanelli, R., Haynes, M.P., Salzer, J.J., Wegner, G., da Costa, L.N. and Freudling, W. (1994), *Astron. J.* **107**, 2036
4. id. (1995), *Astron. J.* submitted
5. Han, M. and Mould, J. (1992), *Ap. J.* **396**, 453
6. Kogut, A. et al. (1993), *ApJ* **419**, 1
7. Lauer, T.R. and Postman, M. (1994), *ApJ* **425**, 418
8. Lilje, P.B. Yahil, A. and Jones, B.T. (1986)*Ap. J.* **307**, 91
9. Lynden–Bell, D., Faber, S.M., Burstein, D., Davies, R.L., Dressler, A., Terlevich, R.J. and Wegner, G. (1988), *Ap. J.* **326**, 19
10. Mathewson, D.S., Ford, V.L. and Buchhorn, M. (1992) *Ap. J. Suppl.* **81**, 413
11. Mathewson, D.S., Ford. V.L. and Buchhorn, M. (1991) *Ap. J. (Letters)* **389**, 1L5
12. Scaramella, R., Baiesi–Pillastrini, G., Vettolani, G. and Chincarini. G. L. (1989) *Nature*, **338**, 562
13. Shaya, E. (1984), *Ap. J.* **280**, 470
14. Strauss, M.A., Davis, M., Yahil, A. and Huchra, J.P. (1992), *Ap. J.* **361**, 49
15. Tammann, G. and Sandage, A. (1985) *Ap. J.* **294**, 81
16. Willick, J. (1991), *Ap. J. (Letters)* **351**, L5